

# Lawrence Berkeley National Laboratory

## Lawrence Berkeley National Laboratory

### Title

Identity of Passive Film Formed on Aluminum in Li-ion Battery Electrolytes with LiPF<sub>6</sub>

### Permalink

<https://escholarship.org/uc/item/1wk1m1ft>

### Authors

Zhang, Xueyuan  
Devine, T.M.

### Publication Date

2008-05-22

Peer reviewed

# Identity of Passive Film Formed on Aluminum in Li-ion Battery Electrolytes with $\text{LiPF}_6$

Xueyuan Zhang<sup>1</sup> and T.M. Devine<sup>1,2</sup>

<sup>1</sup>Lawrence Berkeley National Laboratory  
Energy, Environment and Technology Division

<sup>2</sup>University of California, Berkeley  
Department of Materials Science and Engineering

## Abstract

The passive film that forms on aluminum in 1:1 ethylene carbonate + ethylmethyl carbonate with 1.2M  $\text{LiPF}_6$  and 1:1 ethylene carbonate + dimethyl carbonate with 1.0M  $\text{LiPF}_6$  was investigated by a combination of electrochemical quartz crystal microbalance measurements (EQCM), electrochemical impedance spectroscopy (EIS), and x-ray photoelectron spectroscopy. During anodic polarization of aluminum a film of  $\text{AlF}_3$  forms on top of the air-formed oxide, creating a duplex, or two-layered film. The thickness of the  $\text{AlF}_3$  increases with the applied potential. Independent measurements of film thickness by EQCM and EIS indicate that at a potential of 5.5V vs.  $\text{Li/Li}^+$ , the thickness of the  $\text{AlF}_3$  is approximately 1 nm.

## Introduction

The corrosion resistance of aluminum in organic electrolytes composed of  $\text{LiPF}_6$  dissolved in linear plus cyclized carbonates is exploited in lithium-ion batteries. Although aluminum is resistant to corrosion in battery electrolytes with  $\text{LiPF}_6$ , aluminum is not immune to corrosion. Aluminum serves as the current collector for the battery's cathode and is, in principle, subject to corrosion especially during charging of the batteries. Corrosion of the aluminum current collector is not expected wherever the cathode covers the current collector. However, the cathode is intentionally made porous

in order to increase the cathode/electrolyte interfacial area. Inspections of aluminum current collectors indicate the incidence of corrosion is low but non-negligible, and that the corrosion is localized.<sup>1,2</sup> The localized nature of the corrosion is related to the cathode's through-the-thickness porosity, which exposes to the electrolyte a limited number of small regions of the current collector.

Aluminum current collectors don't corrode at pores in the cathode simply because aluminum is in contact with the electrolyte. In electrochemical tests, aluminum electrodes that are not covered by a cathode are not significantly corroded.<sup>2</sup> A recent study concluded that underdeposit corrosion, which is a type of crevice corrosion, is the most likely mechanism of localized corrosion of aluminum current collectors.<sup>2</sup> That is, aluminum locally corrodes underneath the cathode where electrolyte is trapped in microscopic crevices formed between the porous cathode and current collector.

While aluminum is susceptible to underdeposit corrosion in battery electrolytes with LiPF<sub>6</sub>, aluminum is very resistant to uniform corrosion and pitting corrosion in these same solutions.<sup>1-11</sup> At low potentials (below approximately 4V, according to results presented in the current paper) aluminum is protected against uniform and pitting corrosion by its air-formed oxide,<sup>1,7,8</sup> which is usually < 5 nm thick.<sup>8</sup> At high potentials (above approximately 4V) in LiPF<sub>6</sub>-electrolytes, aluminum is oxidized, but its oxidation results in a solid product that forms on top of the air-formed oxide and protects the aluminum against further corrosion. The identity of the outer layer is the focus of the present paper.

The value in knowing the identity of the outer layer is related to reducing the corrosion of current collectors. Underdeposit corrosion of aluminum current collectors must occur as a consequence of the failure to form the outer layer on top of the air-formed oxide, or as a result of the break down of the outer layer.

If underdeposit corrosion happens because the outer layer of film does not form, then, in order to understand the mechanism of underdeposit corrosion of aluminum current collectors, it is necessary to understand the factors that control formation of the outer layer of film. On the other hand, if underdeposit corrosion occurs by the break down of the outer layer, then, to improve understanding of the mechanism of underdeposit corrosion, it is necessary to understand what contributes to destabilization of the outer layer. In either case, as a first step towards understanding what factors might affect the formation or break down of the outer layer, it is necessary to know the identity of the outer layer.

The present study focuses on identifying the outer layer and a separate inquiry investigates the factors that affect the formation of the outer layer.<sup>12</sup>

The majority of earlier investigations of the film formed on top of aluminum's air-oxide in LiPF<sub>6</sub>/organic carbonate electrolytes have concluded that the film contains fluoride, possibly in the form of AlF<sub>3</sub>,<sup>1,4,6,8-10</sup> but the exact identity of the film remains elusive. In fact, a recent study suggests that the film's key component is phosphorus rather than

fluoride.<sup>11</sup> In our view, the lack of consensus regarding the film's identity is related to the use of only one or two different techniques to probe the film. In the present paper, we investigate the identity of the film formed on aluminum anodically polarized in 1:1 EC+DMC with 1M LiPF<sub>6</sub> and in 1:1 EC+DMC with 1.2M LiPF<sub>6</sub> with three different experimental techniques. Collectively, the results indicate that the protective film is a combination of an inner layer of air-formed oxide and an outer layer of AlF<sub>3</sub>.

## **Experimental Procedure**

### Electrolytes and Samples

Ethylene carbonate (EC, 99%), dimethyl carbonate (DMC), and LiPF<sub>6</sub> (99.99%) were purchased from Alfa, from Grant Chemical (DMC Lot No: 4143600 09100), and from Aldrich, respectively. 1:1 (by volume) EC+DMC with 1.0 M LiPF<sub>6</sub> was prepared in a dry and deoxygenated glove box by mixing the above chemicals in their as received condition. Gen2 electrolyte (1.2 M LiPF<sub>6</sub>/EC+EMC) was purchased from Merck and purified at Quallion.

Electrochemical quartz crystal microbalance (EQCM) experiments were conducted on one micron thick films of aluminum that were sputter deposited onto quartz crystals. Prior to deposition of aluminum, the quartz crystals were coated with a thin film of titanium, which aided adhesion of aluminum. The EQCM aluminum samples were prepared by Maxtek, Inc.

In addition to EQCM experiments, electrochemical impedance spectra were measured for samples of aluminum (99.8%) foil in 1:1 EC+DMC with 1M LiPF<sub>6</sub>. The aluminum foil samples were 0.05 mm thick, circular in shape with an area of 0.5 cm<sup>2</sup>, and were purchased from Aldrich Chemical Co.

Finally, to investigate the electrochemical stability of the battery electrolytes, cyclic polarization curves were measured using platinum as the working electrode. The platinum samples was a 5 mm long wire with a diameter of 1 mm.

Prior to testing, the surfaces of all aluminum and platinum samples were rinsed with acetone.

### Electrochemical Measurements

Multiple anodic polarization scans were conducted on one-micron thick aluminum samples deposited onto 5 MHz quartz crystals (sample's surface area = 1.372 cm<sup>2</sup>). The sample's potential was varied at a sweep rate of 5 mV/s, starting at a potential between 1.8V and 2.5V and finishing at a potential between 5.5V and 7.0V. During each scan, the change in sample's mass was measured simultaneously with the electrochemical cell's current. The EQCM (Model RQCM) was manufactured by Maxtek, Inc. and the sample's potential was controlled by a Gamry Potentiostat (Model PCI 4/750). Lithium from Cyprus Foote Mineral Company was used for reference and counter electrodes.

Electrochemical impedance spectra (EIS) were measured at 2.8V, before and after polarizing the sample to 5.5V, and also at 4.5V for a sample that had been polarized to 5.5V. Electrochemical impedance was measured as a function of frequency by applying to the DC polarized aluminum sample a  $\pm 20$  mV volt signal that varied sinusoidally with time over the frequency range from 10 kHz to 0.01 Hz.

The EIS were obtained using a Solartron 1260 impedance gain-phase analyzer with a Solartron 1286 electrochemical interface. Tests were conducted in a three-electrode Teflon cell with an electrolyte volume of 3 cc, a Li/Li<sup>+</sup> reference electrode, a platinum counter electrode, and a circular aluminum foil sample with a surface area of 0.5 cm<sup>2</sup>.

Cyclic polarization curves (CP) were measured for circular aluminum foil samples (diameter = 8 mm) in a three-electrode Teflon cell with an electrolyte volume of 3 cc. The counter electrode and reference electrode were made of lithium, which was purchased from Cyprus Foote Mineral Company.

After electrochemical testing, the aluminum samples were examined with an optical microscope (50x-500x) for evidence of corrosion.

X-ray photoelectron spectra (XPS) (Phi 5400 ESCA; monochromatic Al K <sub>$\alpha$</sub>  = 1486.6 eV) were measured for the film formed on aluminum that was anodically polarized at 7.0V vs. Li/Li<sup>+</sup> in 1:1 EC+DMC with 1M LiPF<sub>6</sub>.

## Results

### EQCM Tests

Figure 1(a) presents the anodic polarization behavior in Gen 2 of two samples of one-micron thick aluminum sputter deposited onto quartz crystals. The samples are labeled A and B. The changes in mass that occurred during the polarization tests of samples A and B are discussed in the next paragraph. The anodic polarization of sputter-deposited aluminum is a function of the number of anodic scans. The data in Figure 1a compare the anodic polarization behaviors during the first and fourth scans. Similar behavior was detected for both samples. For sample A, when the potential during the first scan reached 4.1V, the anodic current density sharply increased from  $< 1 \mu\text{A}/\text{cm}^2$  and reached its maximum value of  $13.6 \mu\text{A}/\text{cm}^2$  at  $\approx 4.575\text{V}$ .

The total anodic charge passed as the current density of sample A increased to its maximum value of  $13.6 \mu\text{A}/\text{cm}^2$  at a potential of  $4.575\text{V}$  was  $645 \mu\text{Coul}/\text{cm}^2$ . If the total amount of anodic charge were due to oxidative dissolution of aluminum, the mass of aluminum would have decreased by  $60 \times 10^{-9} \text{ gm}/\text{cm}^2$ , which is an amount that is detectable by the EQCM. Furthermore, the amount of oxidization was sufficient that if all of the oxidization current went into formation of a surface film, the increase in mass of the sample would likely be detectable by EQCM.

Figure 1b plots the change in mass of the sputter-deposited aluminum sample A during anodic polarization. Similar results were obtained for the second sample, B. The



measurements of mass change were made concurrently with the measurements of oxidation current presented for both samples in Figure 1a.

From Figure 1b, the mass of Sample A increased by  $\approx 0.12 \mu\text{g}/\text{cm}^2$  as the oxidation current density reached its maximum value at a potential of 4.575V. The mass increase suggests that the anodic current density's sharp increase, which began at  $\approx 4.1\text{V}$ , is related to film formation. The size of the mass increase helps to identify the film.

If the  $645 \mu\text{Coul}/\text{cm}^2$  of charge that is associated with the  $0.12 \mu\text{g}/\text{cm}^2$  mass increase, were entirely associated with film formation, the film would have an mpe (mass per equivalent charge) of 18.0 g/F. In the Discussion, the film will be identified on the basis of its mpe of 18.0 g/F, its elemental composition as provided by XPS, which is presented below, and its electrochemical impedance spectra, which are also presented below. At this point, suffice it to say, the rise in oxidation current between 4.1V and 4.575V (see Figure 1a) is attributed to the formation of a film.

Additional information regarding the reactions that are responsible for the anodic current density on Sample A at potentials above 4.1V is provided by the changes in the electrode's mass, starting at 4.1V and extending to the maximum value of applied potential, 5.5V (see Figures 1a and 1b). While the mpe between 4.1V and 4.575V is 18.2 g/F, the mpe between 4.575V and 5.5V is 14.1 g/F. The decrease in mpe at higher potentials might be due to the formation of a new compound that has a lower mpe than the film that forms at lower potentials. Alternatively, the lower mpe might be due to a

non film-forming oxidation reaction in combination with the same film formation process that occurs at lower potentials.

The occurrence of a non film-forming reaction at high potentials is indicated by the results of the fourth anodic scan of the EQCM experiment presented in Figures 1a and 1b. Starting at approximately 4.5V during the fourth anodic scan the oxidation current starts to slowly increase with increasing potential. The rate of current increase with increasing potential rises sharply at approximately 5.1V. Despite the increases in current, the measurement of mass presented in Figure 1b indicates there is little, if any, change in mass of the aluminum electrode. Since an increase in mass does not accompany the rise in current, the current is not associated with film formation. Possible non-film forming oxidation reactions include oxidation of the electrolyte's components (solvent and/or anion), which becomes more likely the higher the potential. Thus, the lower mpe associated with film formation at high potentials (4.575V to 5.5V) is related to a non film-forming reaction accompanying formation of the same film that forms at lower potentials (4.1V to 4.575V).

Oxidation of the electrolyte is investigated by anodically polarizing platinum and the outcome is presented at the end of the Results section.

In summary, the increase in mass of the aluminum electrode as a result of anodic polarization (Figure 1b) indicates that a film was formed on the surface of aluminum at

potentials above 4.1 V, and at potentials above approximately 4.5V, the film formation is accompanied by a non film-forming oxidation reaction.

The second EQCM experiment and all remaining experiments were conducted in 1:1 EC+EMC with 1.0M LiPF<sub>6</sub>, which is a concentration of LiPF<sub>6</sub> that is slightly less than the concentration of LiPF<sub>6</sub> in Gen 2. The new electrolyte was employed to match the electrolyte used in some batteries,<sup>2</sup> as well as in some earlier studies.<sup>1,10</sup> As shown below, the decrease in concentration of LiPF<sub>6</sub> from 1.2M to 1.0M and the change in solvent from EC+EMC to EC+DMC did not have an effect on the anodic polarization behavior of aluminum.

Figures 2(a,b,c,d) show the results of the second EQCM experiment. The results reproduce the polarization results shown in Figures 1a and 1b, and make clear the effect of potential on film growth. Comparison of Figure 2a with Figure 1a confirms that the anodic polarization behavior of aluminum in 1:1 EC+DMC with 1M LiPF<sub>6</sub> is essentially no different from the anodic polarization behavior in 1:1 EC+EMC with 1.2M LiPF<sub>6</sub>. During the first anodic scan (Figures 2(a,b)), the oxidation rate sharply increases, starting at a potential of  $\approx 4.1V$ . At potentials between 4.1V and 4.632V the electrode's mass increased by only a small amount and the mass increased in an irregular fashion as the potential increased. The total increase in mass ( $0.17 \mu\text{g}/\text{cm}^2$ ) divided by the total charge passed ( $1045 \mu\text{Coul}/\text{cm}^2$ ) as the potential increased from 4.1V to 4.632V yields an mpe of 15.7 g/F, which suggests that the oxidation results in film-formation (and possibly a small amount of electrolyte oxidation).

A constant rate of mass increase starts at 4.632V and the mass continues to increase as the potential is raised to its maximum value of 6.5V (Figure 2b). The mass increased by 0.73  $\mu\text{g}/\text{cm}^2$  and a total of 4483  $\mu\text{Coul}/\text{cm}^2$  was passed as the potential was raised from 4.632V to 6.5V. Dividing the mass increase by the coulombs passed gives an mpe equal to 15.7 g/F, which, in comparison to the mpe of 18.0 g/F measured during anodic polarization between 4.1V and 4.575 V (see Figure 1a), is consistent with film formation and a small amount of electrolyte oxidation.

Second and third anodic scans (not shown) were taken to the same maximum voltage of 6.5V and no change in mass occurred. During a fourth anodic polarization scan (Figures 2(c,d)) the oxidation current and the mass of the electrode increased significantly only after the potential exceeded approximately 6.5V, which is the maximum potential reached in the first anodic scan (Figure 2a), as well as in the second and third (identical) anodic scans (not shown). That the rate of oxidation and the mass increase only after the potential exceeds 6.5V indicates that film growth occurs only when the aluminum is exposed to a higher potential than it has previously experienced.

As already mentioned, the maximum potential during the fourth and final anodic scan was increased from 6.5V, which was the value employed for the first three scans, to 7.0V. As the potential was increased from approximately 6.1V to 7.0V during the final anodic scan, the mass of the electrode increased by 0.095  $\mu\text{g}/\text{cm}^2$  (Figure 2d) and a total of 932  $\mu\text{Coul}/\text{cm}^2$  of charge was passed (Figure 2c). The calculated mpe is 9.8 g/F, which is

significantly less than the values of mpe that occurred at lower potentials. The mpe of 9.8 g/F suggests the formation of a different film than that which formed at lower potentials, or that a greater amount of electrolyte oxidation occurs at the higher potentials, along with formation of the same film that developed at lower potentials. The measurements of mass as a function of applied potential indicate that the rate of mass increase with increasing potential rose sharply at approximately 6.5V, which was the maximum potential applied to the sample in the first three anodic scans. Once again, film growth, as measured by an increase in mass, occurred when the sample was exposed to a potential higher than it had previously experienced.

#### Electrochemical Impedance Spectroscopy

The electrochemical impedance spectra (EIS) presented in Figure 3 provide further evidence of film formation at potentials above approximately 4.0V. The first electrochemical impedance spectrum was obtained at 2.8V, which is the corrosion potential. The sample was then anodically polarized from 2.8V to 5.5V at a rate of 5 mV/s. Following the potentiodynamic polarization, EIS were obtained at 4.5V, and at 2.8V.

The three spectra in Figure 3 are modeled by a resistor in series with a constant phase element (CPE). The CPE is associated with aluminum's surface film. The capacity of the surface film can be obtained from the impedance at 1 Hz. The modulus of the impedance at 1 Hz,  $Z(1 \text{ Hz})$ , in the first spectrum, which was measured at 2.8V, is equal to  $5.63 \times 10^4 \text{ ohm} \cdot \text{cm}^2$ . After potentiodynamic anodic polarization to 5.5V,  $Z(1 \text{ Hz})$

increased to  $7.27 \times 10^4 \text{ ohm} \cdot \text{cm}^2$  and remained at this value when the potential was lowered to 4.5V and to 2.8V. The increase in  $Z(1 \text{ Hz})$  caused by polarization to 5.5V is consistent with the formation of a film at 5.5V. Once formed at 5.5V, the film persists at lower potentials of 4.5V and 2.8V.

The impedance of the CPE is given by  $(2\pi f/f_0)^{-\alpha} C$ , where  $f$  is the frequency in  $\text{s}^{-1}$ ,  $f_0 = 1 \text{ Hz}$ , and  $\alpha$  is measured as 0.88. The capacity at 2.8V is calculated to be  $3.58 \mu\text{F}/\text{cm}^2$  and that at 4.5V is  $12.6 \mu\text{F}/\text{cm}^2$ . The measurements of capacity are employed in the Discussion to estimate the thickness of the film formed on aluminum.

#### X-ray Photoelectron Spectroscopy

The results, presented in Figures 4(a,b), of x-ray photoelectron spectroscopy of aluminum anodically polarized to 7V in Gen 2 indicate the presence of Al bonded to O and Al bonded to F.

Braithwaite et al.<sup>1</sup> measured the XPS of aluminum polarized in 1:1 EC+DMC with 1M  $\text{LiPF}_6$  and obtained results similar to those presented in Figure 4(a, b). In particular, in addition to fluoride and oxygen, the results indicate the presence of carbon and phosphorus.

#### Non-Film-Forming Reactions at Potentials > 4.0V

The anodic polarization behavior of platinum in Gen 2 indicates that a non-film-forming reaction, consisting of oxidation of components of the electrolyte, might occur on

aluminum at potentials  $> 4.0\text{V}$ . The anodic polarization behavior of platinum in Gen 2 is presented in Figure 5. The sharp increase in oxidation current on a platinum electrode at potentials above approximately  $3.5\text{V}$  is presumably the result of oxidation of an electrolyte component. Oxidation of the electrolyte on the platinum electrode suggests that oxidation of the electrolyte might also occur on anodically polarized aluminum at the same time the protective film is forming.

## **Discussion**

### Summary of Key Experimental Results

The increase in mass during the first anodic polarization to  $V_{\text{max}} > 4.1\text{V}$ , and the absence of a mass increase during subsequent polarization scans to the same  $V_{\text{max}}$  (see Figure 1b) indicate the formation of a film on aluminum. The highest measured value of mpe is  $18.2\text{ g/F}$ ; the mpe decreases as the potential increases. The value of  $18.0\text{ g/F}$  is most likely the mpe of the protective film formed on aluminum. The influence of potential on mpe along with the oxidation measured on platinum electrodes polarized above  $3.5\text{V}$  suggest that at high potentials film formation on aluminum is accompanied by electrolyte oxidation. XPS indicates the presence of F, O, C and P on the surface of aluminum anodically polarized at  $7.0\text{V}$ .

In the Discussion, the results are further analyzed in order to determine (1) the identity of the protective film, (2) the thickness of the protective film; and (3) to compare the current results with earlier work.

### Identity of Film Formed on Anodically Polarized Aluminum

It is well-known that a thin film of  $\gamma\text{-Al}_2\text{O}_3$  covers aluminum exposed to air at room temperature.<sup>13</sup> The air-formed surface oxide is responsible for aluminum's resistance to corrosion in 1:1 EC+DMC with 1M LiPF<sub>6</sub> at potentials less than approximately 4.0V (see Figure 1a). In a separate study we demonstrate that aluminum, which has a standard reduction potential of 1.38 V vs Li/Li<sup>+</sup> (Li/Li<sup>+</sup> = -3.05 v. SHE), is oxidized at potentials as low as 1.0 V when mechanically stripped of its air-formed oxide.<sup>12</sup> The impedance spectrum of aluminum immersed in 1:1 EC+DMC with 1M LiPF<sub>6</sub> (Figure 3) indicates the air-formed film on aluminum is approximately 1.2 nm to 2.4 nm thick (see Appendix I), which is in good agreement with the thickness of 2 nm-4 nm estimated in earlier studies using Auger electron spectroscopy and XPS.<sup>14,15</sup>

As mentioned in the Results section, the EQCM measurements of the polarization behavior of aluminum with its air-formed surface oxide during anodic polarization from a lower limit of 1.5V or 2.5V to an upper limit that ranges from 5.5V in Gen2 (Figure 1a) to 6.5V (Figure 2a) and 7.0V (Figure 2c) in 1:1 EC+DMC with 1M LiPF<sub>6</sub> suggests that a protective film is formed on top of the air-formed film. In particular, the oxidation rate during the second-fourth scans to the same maximum voltage is considerably lower than during the first scan.

The identity of the protective film is revealed by the combined results of EQCM and XPS. Table I summarizes the influence of potential on the mpe during film formation. In



general, as the maximum applied potential increases, the mpe decreases. As already mentioned in the Results section and as is discussed below, the decrease in mpe with maximum applied voltage is attributed to the occurrence of non film-forming reactions at high values of potential (i.e.,  $\geq 4.5\text{V}$ ). Therefore, the mpe associated primarily, if not solely, with film formation is 18.0 g/F, which was measured during polarization between 4.1 and 4.575 V (the lowest values of voltage in which a mass increase was measured; see Figures 1a and 1b).

The mpe of 18.0 g/F is close to the mpe of  $\text{AlF}_3$ , 19.0 g/F. The combination of the mpe of 18.0 g/F and the strong fluoride peak in the XP spectrum of the sample polarized to 7.0V (see Figure 4(a,b)) strongly suggest that the oxidation of aluminum forms a film of  $\text{AlF}_3$ .

The  $\text{O}^-$  peak in the XP spectrum suggests that the air-formed film is still present on the aluminum and that the  $\text{AlF}_3$  layer forms on top of the air-formed oxide.

#### Comparison of Present Results with Earlier Results

Morita et al.<sup>10</sup> indicated that  $\text{Al}(\text{OH})_3$  and  $\text{Al}_2\text{O}_3$ , as well as  $\text{AlF}_3$ , formed during anodic polarization of aluminum in 1:1 EC+DMC with 1M  $\text{LiPF}_6$ . Presumably, the formation of  $\text{Al}(\text{OH})_3$  (mpe = 17 g/F) and  $\text{Al}_2\text{O}_3$  (mpe = 8 g/F) is a consequence of water contamination of the electrolyte. In the present study, the water concentration was < 1 ppm (measured by Karl Fischer Titration) and it is unlikely that a significant amount of hydroxide or oxide would form.

Note that phosphorus and carbon are also present in the XP spectra in Figure 4a. The detection of phosphorus duplicates the finding of Braithwaite et al.<sup>1</sup> The presence of phosphorus is consistent with the suggestion of Zhang and Jow<sup>7</sup> that phosphorus, and not fluoride, is the key element in the protective film formed on aluminum. However, the mpe values measured in this study range from 18.0 g/F at low potentials to 9.8 g/F at high potentials and, in our view, are best explained by the formation of  $\text{AlF}_3$ , accompanied at higher potentials by electrolyte oxidation (see below).

Table II summarizes the results of a number of earlier investigations of the film that forms on aluminum during anodic polarization in electrolytes composed of organic carbonates with  $\text{LiPF}_6$ . The results indicate a range in the critical value of potential above which the film forms. Some of the scatter is due to the different voltage sweep rates that were employed by different investigators. Generally, the higher critical potentials were measured using higher sweep rates (e.g., 50 mV/s). After accounting for the effect of sweep rate, most of the reported values of critical potential (column 4, Table II) are close to the value of 4.0V measured in the present study. Most studies have concluded that the film that forms on aluminum consists in whole, or in part, of  $\text{AlF}_3$  (column 5, Table II). In the earlier studies, the evidence for  $\text{AlF}_3$  mostly came from XPS measurements of the film. The present EQCM results complement the earlier results by combining EQCM and EIS with XPS.

Other investigators, which employed salts other than, or in addition to,  $\text{LiPF}_6$  (see rows 7 and 9 of Table II), have proposed that the film of  $\text{AlF}_3$  forms from the air-formed oxide film. In films formed on aluminum anodically polarized in electrolytes with a mixed salt of  $\text{LiCF}_3\text{SO}_3 + \text{LiPF}_6$  Nakajima et al.<sup>9</sup> proposed that the fluoride ion that forms the  $\text{AlF}_3$  comes from the oxidation of  $\text{CF}_3\text{SO}_3^-$  and that other products of the oxidation of  $\text{CF}_3\text{SO}_3^-$  reduce the air-formed  $\text{Al}_2\text{O}_3$  to Al.  $\text{F}^-$  then reacts with Al to form  $\text{AlF}_3$ . Kanamura et al.<sup>8</sup> proposed that when 0.01M HF is added to the organic electrolyte composed of PC with  $\text{LiCF}_3\text{SO}_3$  and  $\text{Li}(\text{CF}_3\text{SO}_2)_2$ , the air formed film of  $\text{Al}_2\text{O}_3$  is converted to AlOF and  $\text{AlF}_3$ . Collectively, the present results of EIS and EQCM indicate that during anodic polarization of aluminum in 1:1 EC+DMC with 1M  $\text{LiPF}_6$ , a film of  $\text{AlF}_3$  forms on top of the air-formed oxide, and that the formation of  $\text{AlF}_3$  does not involve the decomposition of the air-formed film. That is, if  $\text{AlF}_3$  (mpe = 19.0 g/F) formed at the expense of  $\text{Al}_2\text{O}_3$  (mpe = 8.0 g/F), the net mpe would be considerably smaller than the measured value of 18.0 g/F. Thus, the film on aluminum that is anodically polarized in 1:1 EC+DMC with 1M  $\text{LiPF}_6$  is a duplex film consisting of an inner layer of air-formed  $\text{Al}_2\text{O}_3$  and an outer layer of  $\text{AlF}_3$ .

#### Thickness and Protectiveness of $\text{AlF}_3$

As mentioned in the Results, the capacitance of aluminum, covered with its air-formed oxide, is  $3.6 \mu\text{F}/\text{cm}^2$ , which suggests the thickness of the air-formed film is approximately 1.2 nm to 2.5 nm. Anodic polarization of aluminum to 5.5V increases the capacitance to  $12.6 \mu\text{F}/\text{cm}^2$ . Assuming the increased capacitance is due to formation of

AlF<sub>3</sub> on top of the air-formed oxide, the thickness of the AlF<sub>3</sub> is equal to 1.0 nm (see Appendix II).

The EQCM measurements provide a second estimate of the thickness of the AlF<sub>3</sub> film that forms on top of the air-formed oxide (see Appendix II). Using the density of AlF<sub>3</sub> (= 2.882 g/cc), the film formed at 5.5V is 1.2 nm thick, which agrees well with the thickness of 1.0 nm estimated from capacity measurements.

Although the AlF<sub>3</sub> film is only approximately 1 nm thick, it significantly adds to the corrosion resistance of the air-formed oxide. In a separate study, the additional corrosion protection provided by the AlF<sub>3</sub> is demonstrated by the significant increase in aluminum's resistance to pitting corrosion in 1:1 EC+DMC with 1M LiTFSI.<sup>12</sup>

The layer of AlF<sub>3</sub> that forms on top of the air-formed oxide is crucial for the corrosion resistance of aluminum current collectors. Based on the corrosion performance of aluminum in a number of electrolytes, both aqueous and nonaqueous, the air-formed oxide should not be expected to protect aluminum against oxidation at voltages much higher than approximately 4 V vs. Li/Li<sup>+</sup>. For example, in aqueous solutions of 1M NaNO<sub>3</sub>, 1M KSCN, and 1M NaCl, pitting corrosion of aluminum starts at potentials of 5.0V, 4.5V, and 2.6V, respectively.<sup>18</sup> In aqueous 10M H<sub>2</sub>SO<sub>4</sub> and aqueous 12M H<sub>3</sub>PO<sub>4</sub>, aluminum uniformly oxidizes,<sup>19</sup> forming an anodized surface film, at potentials above approximately 4.5V vs Li/Li<sup>+</sup>. In non-aqueous solutions, such as 1:1 EC+DMC with 1M LiTFSI, the air-formed oxide on aluminum breaks down at potentials around 4.0V and

the aluminum suffers significant pitting corrosion.<sup>5,6,8,20-22</sup> Consequently, it is no surprise that aluminum, which is protected only by its air-formed oxide, is susceptible to oxidation at potentials above 4.0V in 1:1 EC+DMC with 1M LiPF<sub>6</sub>.

Aluminum current collectors might experience potentials as high as 4.2V during battery charging. From the perspective of maintaining a functioning cathode in Li-ion batteries, it is fortunate that aluminum's oxidation produces AlF<sub>3</sub>, which is sufficiently insoluble in EC+DMC that it forms as a protective layer on top of the air-formed oxide. In contrast, AlF<sub>3</sub> is reasonably soluble in aqueous solutions so that even very dilute aqueous solutions of HF (e.g., 0.001M) cause very severe corrosion of aluminum.<sup>14</sup>

#### Electrolyte Oxidation at High Potentials

Finally, consider the possible reasons why the mpe associated with film formation on aluminum decreases as the applied potential during anodic polarization of aluminum increases (see Table I). In principle, the decreasing value of mpe could be due to either the formation of films other than AlF<sub>3</sub> and with lower mpe, or the formation of AlF<sub>3</sub> along with electrolyte oxidation. Since XPS of aluminum polarized to the high potential of 7.0V exhibited strong peaks for F<sup>-</sup>, which is attributed to AlF<sub>3</sub>, and O<sup>-</sup>, which is assigned to Al<sub>2</sub>O<sub>3</sub>, the decreasing value of mpe is not associated with a change in the film that forms. In addition, possible films, other than AlF<sub>3</sub>, with mpe < 19 g/F include AlOF (mpe = 11 g/F) and Al<sub>2</sub>O<sub>3</sub> (mpe = 8 g/f). However, AlOF and Al<sub>2</sub>O<sub>3</sub> seem unlikely to form because there is insufficient water. Also, the anodic polarization of platinum (see Figure 5) indicates that the electrolyte can be oxidized at low potentials on platinum,

which opens up the possibility of electrolyte oxidation at higher potentials on aluminum covered with air-formed oxide plus  $\text{AlF}_3$ . The carbon and phosphorus peaks in the XPS of the film formed on aluminum that was anodically polarized to 7.0V might belong to products of the electrolyte's oxidation.

The solvents of EC+DMC and EC+EMC are the components of the electrolyte that are most likely oxidized at relatively low potentials (e.g., above approximately 4.5V).<sup>23-25</sup> The oxidation potential of the anion  $\text{PF}_6^-$  was measured as 4.94V (on the surface of a glassy carbon electrode).<sup>26</sup> Hence, oxidation of  $\text{PF}_6^-$  is unlikely to occur on the surface of platinum at potentials as low as 3.5V and on aluminum at potentials approximately equal to 4.5V.

### **Summary and Conclusions**

The results presented in this paper indicate that a protective film is formed on aluminum when anodically polarized in 1:1 EC+EMC with 1.2M  $\text{LiPF}_6$  and in 1:1 EC+DMC with 1.0M  $\text{LiPF}_6$ . Film formation starts at potentials around 4.1V. The amount of the film increases with increasing applied potential.

Results of EQCM experiments indicate the film formation is characterized initially by an mpe of 18.0 g/F and at higher potentials by an mpe of 9.8 g/F. The most likely explanation for an mpe of 18.0 g/F is that the oxidation of aluminum produces a film of  $\text{AlF}_3$  (mpe = 19.0 g/F). EIS support the view that oxidation of aluminum produces a film of  $\text{AlF}_3$ . Based on impedance measurements the surface of aluminum is initially covered

with a 1.2 nm to 2.4 nm thick layer of air-formed  $\text{Al}_2\text{O}_3$ . Anodic polarization to 5.5V increases the impedance and is consistent with the formation (on top of air-formed  $\text{Al}_2\text{O}_3$ ) of a thin layer of  $\text{AlF}_3$ . Based on electrode's increase in mass, the film of  $\text{AlF}_3$  is estimated to approximately 1 nm thick..

The formation of  $\text{AlF}_3$  is further supported by the results of the film's XP spectrum, which indicated the presence of fluoride ions. An mpe of 9.8 g/F, which occurs at higher potentials, is likely the result of at least two reactions: (1) formation of a film of  $\text{AlF}_3$  and (2) oxidation of the electrolyte. Electrolyte oxidation occurred at low potentials on platinum, and suggests, but does not prove, that electrolyte oxidation might compose some or all of the non-film-forming reactions that accompany protective film formation on aluminum.

## **Acknowledgments**

This work was supported by the Assistant Secretary for Energy Efficiency and Renewable Energy, Office of FreedomCAR and Vehicle Technologies U.S. Department of Energy under Contract No. DE-AC03-76SF00098.



## Appendix I

### Thickness of Air-Formed Oxide

The thickness of the air-formed oxide on aluminum and the thickness of the  $\text{AlF}_3$  that forms on top of the air-formed oxide are estimated from the EIS (Figure 3). The impedance spectra are modeled by a constant phase element in series with a resistance. The constant phase element represents the impedance associated with aluminum's surface film. The impedance of the CPE is given by  $1/[2\pi f/f_0]^\alpha C$ , and  $C$  is assigned to the capacitance of the surface film,  $C = \epsilon\epsilon_0/d_{\text{film}}$ , where  $\epsilon$  is the film's dielectric constant and  $d_{\text{film}}$  is the film's thickness.

An air-formed film of  $\text{Al}_2\text{O}_3$ , which has a dielectric constant of between 5 and 10,<sup>14</sup> is assumed to cover the aluminum surface. The impedance at 1 Hz measured at the open circuit potential of 2.8V (see Figure 3) consists of the modulus of the impedance, which equals  $5.63 \times 10^4 \text{ ohm}\cdot\text{cm}^2$ , and the phase angle of  $77.3^\circ$ . The calculated value of the capacitive impedance is  $5.49 \times 10^4 \text{ ohm}\cdot\text{cm}^2$  and indicates the thickness of the air-formed oxide is between 1.2 and 2.5 nm. The range in thickness is due to the range in possible values of the air-formed oxide's dielectric constant. The calculated thickness of the air-formed film is in good agreement with earlier measurements with Auger electron spectroscopy (AES) and EIS, which indicate that the thickness of the air-formed film on aluminum is in the range of 2-4 nm.<sup>14,15</sup>

## Appendix II

### Thickness of AlF<sub>3</sub>

Assuming that a duplex film, consisting of the air-formed Al<sub>2</sub>O<sub>3</sub> plus an outer layer of AlF<sub>3</sub>, which has a dielectric constant of 2.2,<sup>16</sup> is present on the aluminum surface anodically polarized to 5.5V, the CPE's measured impedance (Figure 3) provides an estimate of the thickness of the AlF<sub>3</sub> layer. The modulus of the impedance is  $7.27 \times 10^4$  ohm•cm<sup>2</sup> and the phase angle is 77.3° at a frequency of 1 Hz. The capacitive impedance is, therefore, 70,919 ohm•cm<sup>2</sup>. For a constant phase element with  $\alpha = 0.88$ , the capacitance associated with the impedance is 2.8 μCoul/cm<sup>2</sup>. The capacitance of 2.8 μCoul/cm<sup>2</sup> is assumed to result from the capacitance of the air-formed oxide (3.6 μCoul/cm<sup>2</sup>) in series with the capacitance of the AlF<sub>3</sub>. Consequently, the capacitance of the AlF<sub>3</sub> is 12.6 μCoul/cm<sup>2</sup>.

A capacitance of 12.6 μCoul/cm<sup>2</sup> associated with a film whose dielectric constant is 2.2, suggests the thickness of the film is 0.14 nm. The film's estimated thickness is very thin and calls into question the validity of the assumptions that the film is of uniform thickness and/or that the film's dielectric constant is 2.2. We conclude that the film is thin and might not be uniformly thick, and that the measurement of capacitance does not provide a reliable estimate of the film's thickness.

The thickness of the layer of AlF<sub>3</sub> can also be estimated from the EQCM data in Figure 1b. When anodically polarized from approximately 4.1V to 5.5V the mass of the

aluminum electrode was increased by  $0.4 \mu\text{g}/\text{cm}^2$ . Assuming the density of  $\text{AlF}_3$  is  $2.882 \text{ g}/\text{cc}$ ,<sup>17</sup> the thickness of the  $\text{AlF}_3$  formed by anodic polarization to  $5.5\text{V}$  is  $1.4 \text{ nm}$ .

Collectively, the EQCM and EIS results suggest a thin film of  $\text{AlF}_3$ , which is approximately  $1 \text{ nm}$  thick, forms on top of an air-formed oxide that is  $1.2 - 2.5 \text{ nm}$  thick, when aluminum is anodically polarized to  $+5.5\text{V}$ .

## References

1. J.W. Braithwaite, A. Gonzales, G. Nagasubramanian, S.J. Lucero, D.E. Peebles, J.A. Ohlhausen, and W.R. Cieslak, *J. Electrochemical Soc.*, **146**, p. 448 (1999).
2. Xueyuan Zhang, B. Winget, M. Doeff, J.W. Evans and T.M. Devine, *J. Electrochemical Soc.*, **152**, p. B448 (2005).
3. K. Kanamura, T. Okagawa, Z. Takehara, *J. Power Sources*, **57**, 119 (1995).
4. C. Iwakura, Y. Fukumoto, H. Inoue, S. Ohashi, S. Kobayashi, H. Tada and M. Abe, *J. Power Sources*, **68**, 301 (1997).
5. H. Yang, K. Kwon, T.M. Devine, and J.W. Evans, *J. Electrochem. Soc.*, **147**, 4399 (2000).
6. Xianming Wang, E. Yasukawa, S. Mori, *Electrochimica Acta*, **45**, 2677 (2000).
7. S.S. Zhang, T.R. Jow, *J. Power Sources*, **109**, 458 (2002).
8. K. Kanamura, T. Umegaki, S. Shiraishi, M. Ohashi, and Z. Takehara, *J. Electrochem. Soc.*, **149**, A185 (2002).
9. T. Nakajima, M. Mori, V. Gupta, Y. Ohzawa, and H. Iwata, *Solid State Sciences*, **4**, 1385 (2002).
10. M. Morita, T. Shibata, N. Yoshimoto, and M. Ishikawa, *Electrochimica Acta*, **47**, 2787 (2002).
11. S.S. Zhang, K. Yu, T.R. Jow, *J. Electrochem. Soc.*, **149**, A586 (2002).
12. Xueyuan Zhang and T.M. Devine, "Factors That Influence Formation of  $\text{AlF}_3$  Passive Film on Aluminum in Li-ion Battery Electrolytes with  $\text{LiPF}_6$ ." Submitted for publication in the *Journal of the Electrochemical Society*.

13. P.V. Thomas, V. Ramakrishnan, V.K. Vaidyan, *Thin Solid Films*, **170**, p. 35 (1989).
14. J.R. Scully, "Characterization of the Corrosion of Aluminum Thin Films Using Electrochemical Impedance Methods," p. 276 in *Electrochemical Impedance: Analysis and Interpretation, ASTM STP 1188*, J.R. Scully, D.C. Silverman, and M.W. Kendig, Eds., American Society for Testing Materials, Philadelphia (1993).
15. J.R. Scully, R.P. Frankenthal, K.J. Hanson, D.J. Siconolfi, and J.D. Sinclair, *J. Electrochem. Soc.*, **137**, p.1365 (1990).
16. Table of Dielectric Constants. ASI Instruments Web Site.  
<http://www.asiinstr.com/technical/Dielectric%20Constants.htm>.
17. *CRC Handbook of Chemistry and Physics, 65<sup>th</sup> ed.*, R.C. Weast, M.J. Astle, W.H. Beyer, eds. P.B68, CRC Press, Inc. Boca Raton, Fl. (1985).
18. J.R. Galvele, S.M. de De Micheli, I.L. Muller, S.B. deWexler, I.L. Alanis, in *Localized Corrosion*, R.W. Staehle, B.F. Brown, J. Kruger, A. Agrawal, eds., p.580, NACE, Houston, TX (1986).
19. *ibid.*, p.597
20. L. J. Krause, L.V. Lamanna, J. Summerfield, M. Engle, G. Korba, R. Loch, R. Atanasoski, *J. Power Sources*, **68**, 320 (1997).
21. W.K. Behl and E.J. Plichta, *J. Power Sources*, **72**, p.132 (1998)
22. Seung-Wan Song, T.J. Richardson, G.V. Zhuang, T.M. Devine, J.W. Evans, *Electrochimica Acta*, **49**, p.1483 (2004).
23. E.J. Plichta and W.K. Behl, *J. Power Sources*, **88**, p.192 (2000).
24. F. Joho and Petr Novak, *Electrochimica Acta*, **45**, p. 3589 (2000).

25. M. Moshkovich, M. Cojocaru, H.E. Gottlieb, D. Aurbach, *J. Electroanalytical Chem.*, **497**, p. 84 (2001).
26. V.R. Koch, L.A. Dominey, C. Nanjundiah, M.J. Ondrechen, *J. Electrochem. Soc.*, **143**, p. 798 (1996).

**Table I**

Influence of Potential on Value of MPE

<u>Figure</u>	<u>Electrolyte</u>	<u><math>V_i \rightarrow V_{max}</math></u>	<u><math>i_{max}(\mu A/cm^2)</math></u>	<u>mpe(g/F)</u>
1a/1b	1.2M LiPF <sub>6</sub> in 1:1 in EC+EMC	4.1V->4.575V	13.57	18.0
1a/1b	1.2M LiPF <sub>6</sub> in 1:1 in EC+EMC	4.575V->5.5V	11	14.1
2a/2b	1.0M LiPF <sub>6</sub> in 1:1 in EC+DMC	4.0V->4.632V	16.54	15.7
2a/2b	1.0M LiPF <sub>6</sub> in 1:1 in EC+DMC	4.632V->6.5V	12	15.7
2c/2d	1.0M LiPF <sub>6</sub> in 1:1 in EC+DMC	6.068V->7.0V	10	9.8

Table II Investigations of Surface Films Formed on Aluminum in Electrolytes with LiPF<sub>6</sub>

Salt	Solvent	Reference	Critical Potential	Main Results
LiPF <sub>6</sub> LiN(SO <sub>2</sub> CF <sub>3</sub> ) <sub>2</sub>	1:1 EC+DME	X. Wang et al. <sup>6</sup>	≥ 4.0 V increases with [LiPF <sub>6</sub> ]	Prot. film contains AlF <sub>3</sub> . F <sup>-</sup> from decomp of PF <sub>6</sub> <sup>-</sup> .
LiPF <sub>6</sub>	PC	Kanamura et al. <sup>3</sup>	≈4.2V (50 mV/s)	Prot. film formed at 5.5V/1h contains AlF <sub>3</sub> . AlF <sub>3</sub> identified by XPS.
LiPF <sub>6</sub>	1:1 PC+DEC and EC+DMC	Braithwaite et al. <sup>1</sup>	>3.7V (voltage sweep rate not specified)	Film mainly determined by LiPF <sub>6</sub> . Binding Energy (XPS) of F <sup>-</sup> in film => film ≠ metal fluoride.
LiPF <sub>6</sub>	EC+DME	Zhang and Low <sup>7</sup>	≥ 3.8 V (5 mV/s)	More stable film formed in EC+DMC than in EC+ DME
LiPF <sub>6</sub>	PC	Yang et al. <sup>5</sup>	≥6V (50 mV/s) scratched electrode	Prot. film forms in xM LiPF <sub>6</sub> + (1-x)M LiN(CF <sub>3</sub> SO <sub>2</sub> ) <sub>2</sub> for x = 0.5 but not for x = 0.1.
LiPF <sub>6</sub>	PC	Kanamura et al. <sup>8</sup>	≈ 4.3 V (5 mV/s)	Oxidation above 4.3V forms protective film
LiCF <sub>3</sub> SO <sub>3</sub> Li(CF <sub>3</sub> SO <sub>2</sub> ) <sub>2</sub>	PC	Kanamura et al. <sup>8</sup>	≈ 5.3V (10 mV/s)	Small amt. of F <sup>-</sup> through- out film is from oxidation of CF <sub>3</sub> SO <sub>3</sub> <sup>-</sup> . 0.01M HF changes film from air-formed Al <sub>2</sub> O <sub>3</sub> to AlF <sub>3</sub> and AlOF. 0.01M HF decreases amt. of pitting and is assoc. with prot. film.
LiPF <sub>6</sub>	EC+DEC	Iwakura et al. <sup>4</sup>	≈4.0V (5 mV/s)	F <sup>-</sup> detected by XPS in prot. film
LiCF <sub>3</sub> SO <sub>3</sub> + LiPF <sub>6</sub>	EC+DEC	Nakajima et al. <sup>9</sup>	≈4.0V (10 mV/s)	Products of oxidation of CF <sub>3</sub> SO <sub>3</sub> <sup>-</sup> reduce air- formed Al <sub>2</sub> O <sub>3</sub> to Al. Oxidation of complex fluoride anion creates highly reactive F and F <sup>-</sup> , which react with bare Al to form prot. film.
LiPF <sub>6</sub>	EC+DMC	Morita et al. <sup>10</sup>	3.0V (10 mV/s)	Prot. film, mpe = 30g/F. XPS=> prot. film = AlF <sub>3</sub>



				+ Al <sub>2</sub> O <sub>3</sub> + Al(OH) <sub>3</sub> .
--	--	--	--	--

## List of Figures

Figure 1a. First and fourth anodic polarization scans of two, sputter-deposited thin films of aluminum in Gen 2 electrolyte.

Figure 1b. Change in mass of sputter-deposited thin film of aluminum (Sample A) during the first and fourth anodic polarization scans in Gen 2 electrolyte.

Figure 2a. First anodic polarization scan from 2.5V to 6.5 V of sputter deposited thin film of aluminum in 1:1 EC+DMC with 1M LiPF<sub>6</sub>.

Figure 2b. Change in mass of sputter-deposited, thin film of aluminum during the first anodic polarization scan in 1:1 EC+DMC with 1M LiPF<sub>6</sub> (same scan as in Figure 2a).

Figure 2c. Fourth anodic polarization scan from 2.5V to 7.0 V of sputter deposited thin film of aluminum in 1:1 EC+DMC with 1M LiPF<sub>6</sub>.

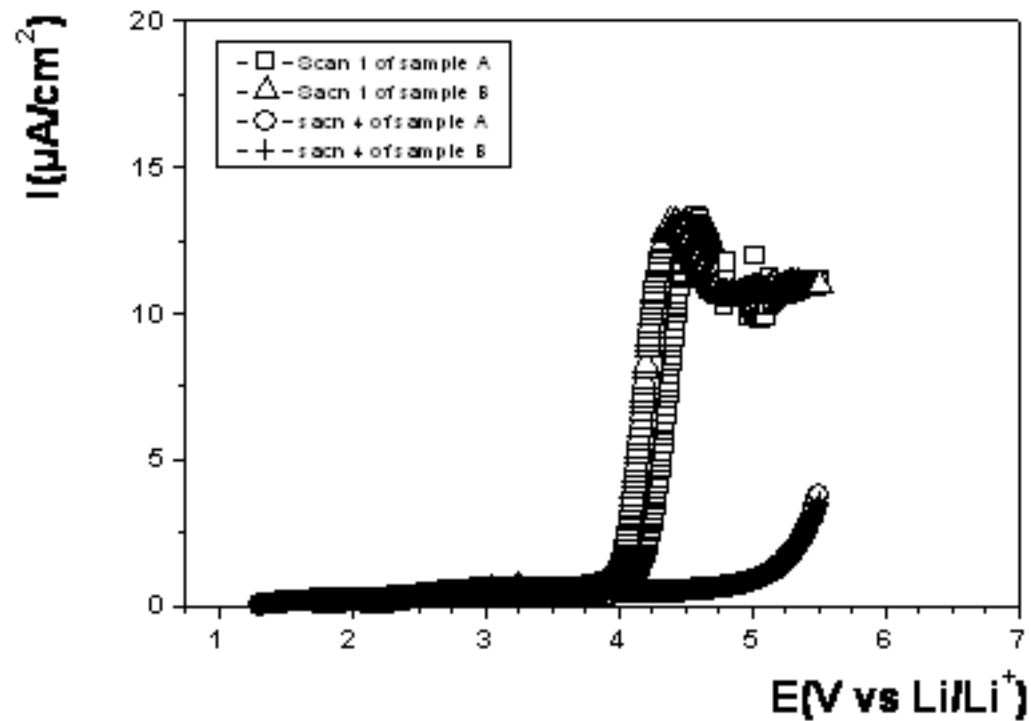
Figure 2d. Change in mass of sputter-deposited, thin film of aluminum during the fourth anodic polarization scan in 1:1 EC+DMC with 1M LiPF<sub>6</sub> (same scan as in Figure 2c).

Figure 3. Bode plot of electrochemical impedance of aluminum in Gen 2 electrolyte (1) at 2.8V in the as-immersed condition, (2) at 4.5 V following polarization to 5.5 V, and (3) at 2.8 V following polarization to 5.5 V.

Figure 4a. XPS spectrum of aluminum after anodic polarization in Gen 2 from OCP to 7.0 V vs Li/Li<sup>+</sup>.

Figure 4b. XPS spectrum of Al 2p for aluminum sample after anodic polarization in Gen 2 from OCP to 7.0 V vs Li/Li<sup>+</sup>.

Figure 5. Fourth anodic polarization scan of platinum in 1:1 EC+DMC with 1M LiPF<sub>6</sub>.



**Figure 1a. First and fourth anodic polarization scans of two, sputter deposited, thin films of aluminum in Gen 2 electrolyte**

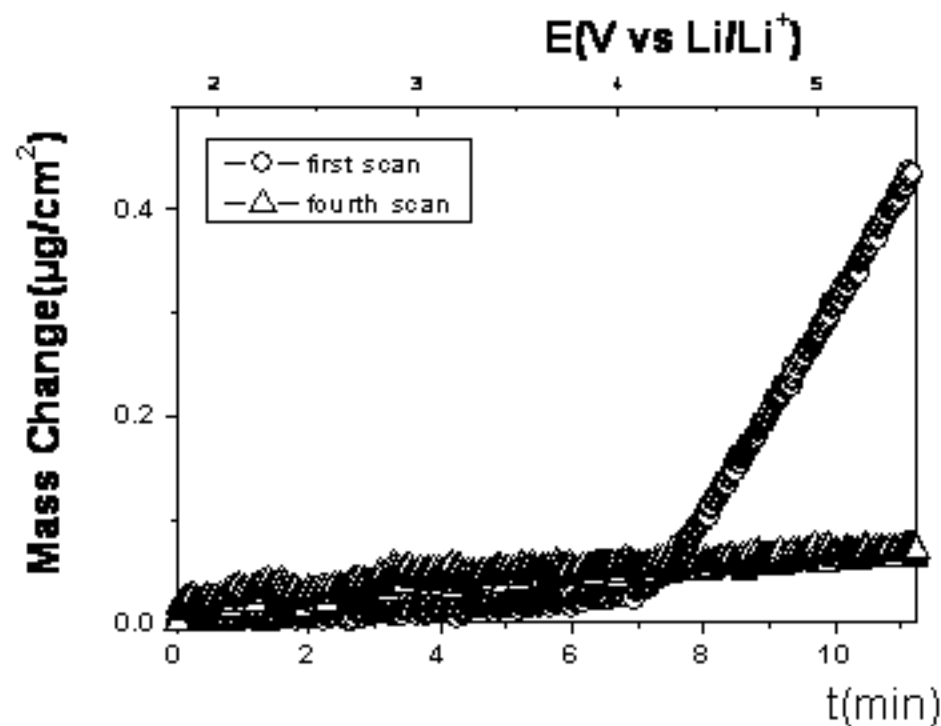


Figure 1b. Change in mass of sputter-deposited, thin film of aluminum (sample A) during the first and fourth anodic polarization scans in Gen 2 electrolyte

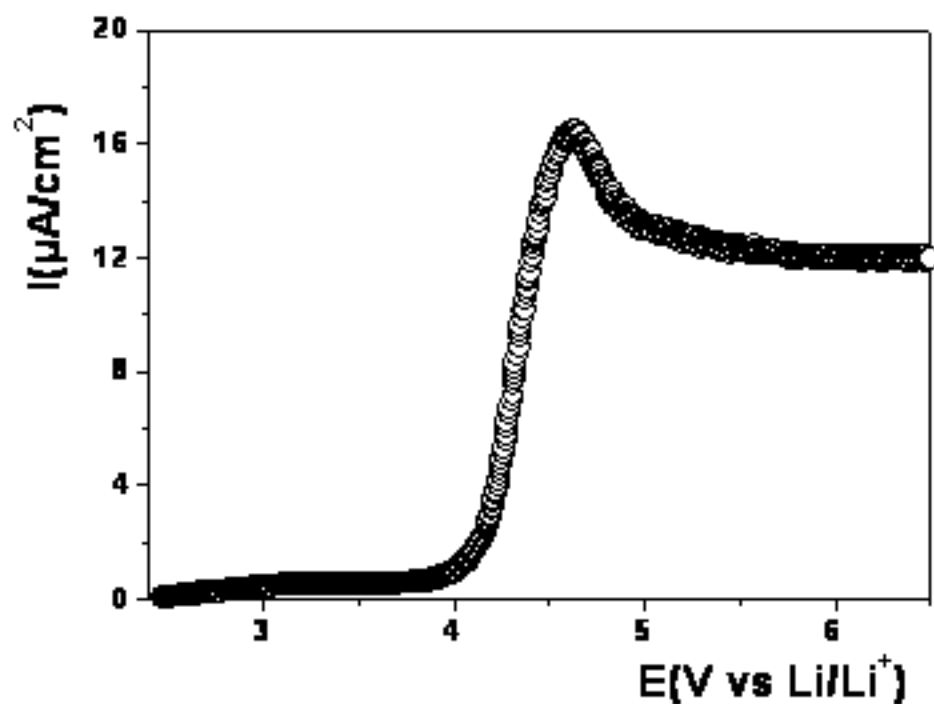


Figure 2a. First anodic polarization scan from 2.5V to 6.5V of sputter deposited, thin film of aluminum in 1:1 EC+DMC with 1M  $\text{LiPF}_6$ .

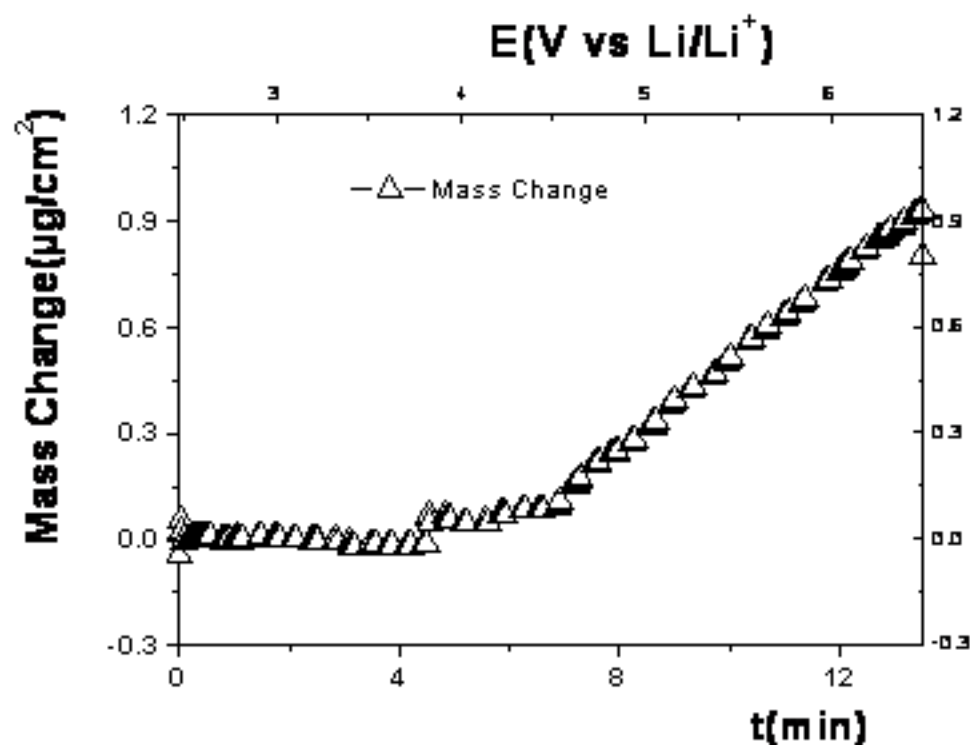
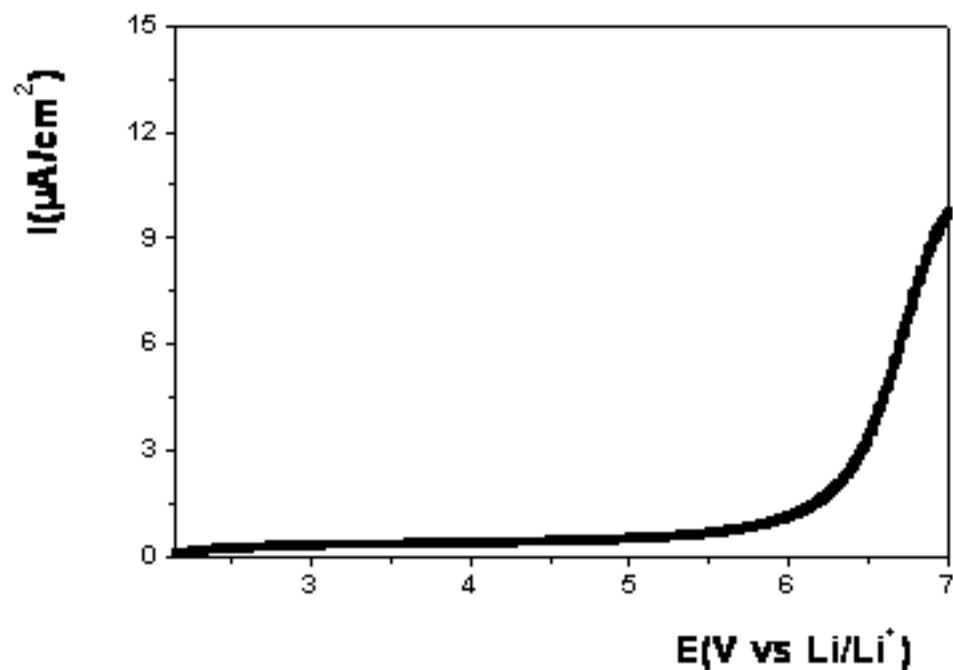


Figure 2b. Change in mass of sputter-deposited, thin film of aluminum during the first anodic polarization scan in 1:1 EC+DMC with 1M LiPF<sub>6</sub> (same scan as in Figure 2a).



**Fig 2c. Fourth anodic polarization scan from 2.5V to 7V of sputter deposited, thin film of aluminum in 1:1 EC+DMC with 1M  $\text{LiPF}_6$ .**



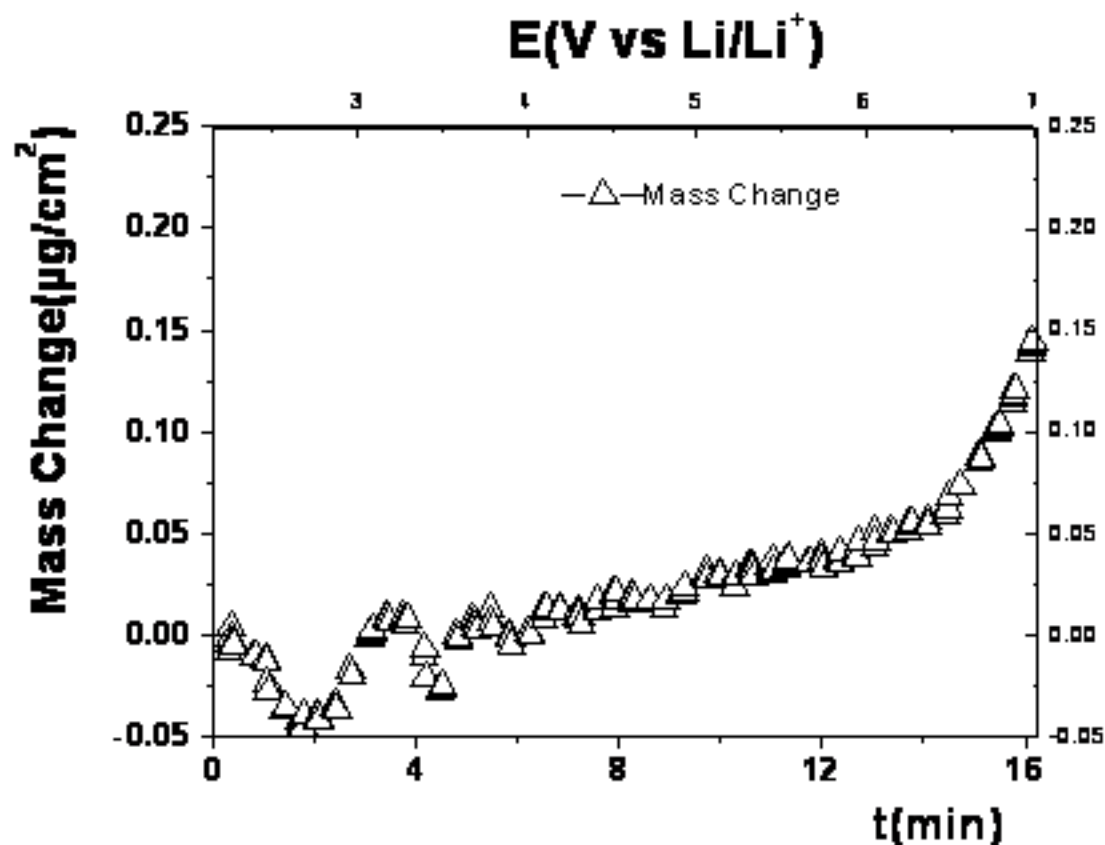
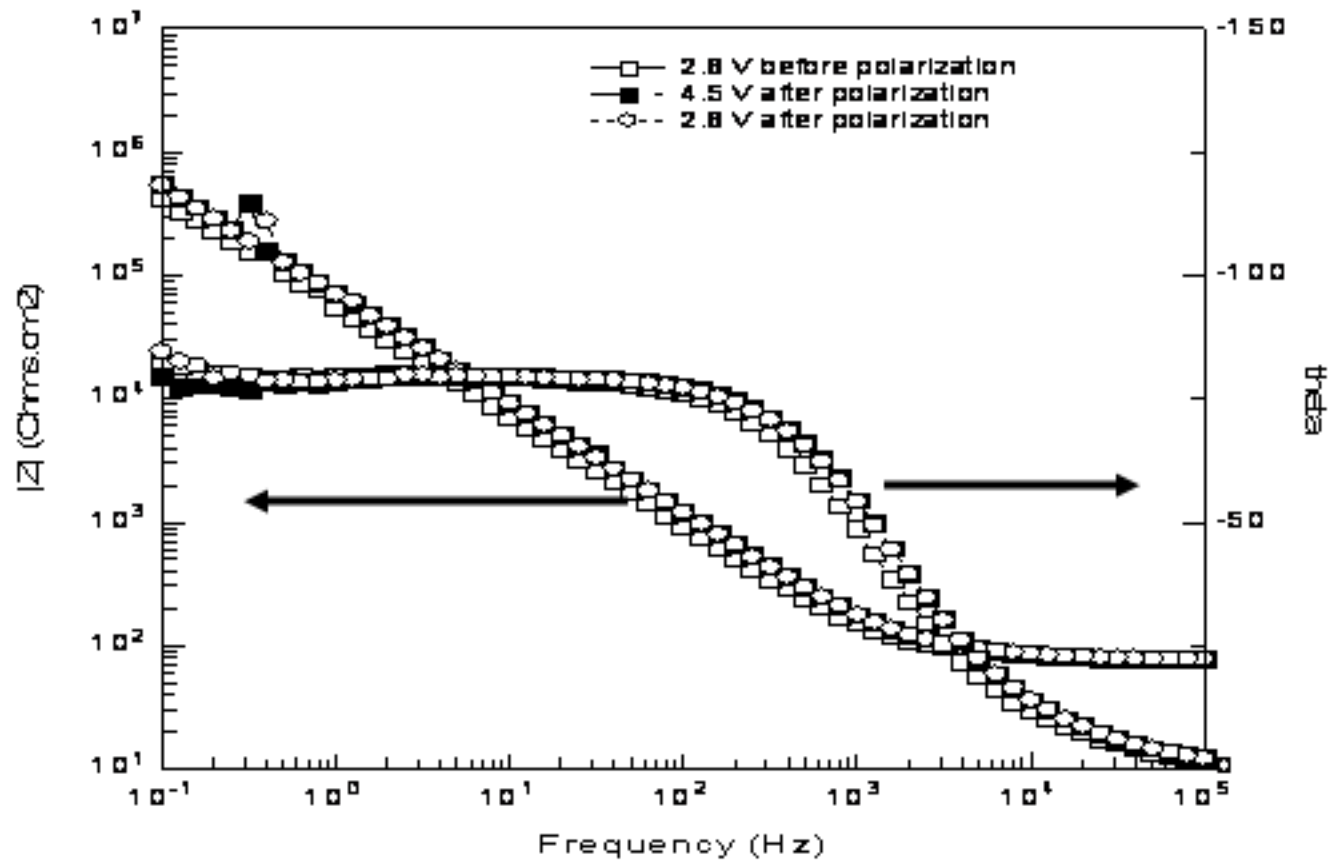


Figure 2d. Change in mass of sputter-deposited, thin film of aluminum during the fourth anodic polarization scan in 1:1 EC+DMC with 1M  $LiPF_6$  (same scan as in Figure 2c).



**Fig 3. Bode plot of electrochemical impedance of aluminum in Gen 2 electrolyte (1) at 2.8V in the as-immersed condition, and (2) at 4.5V following polarization to 5.5V, and (3) at 2.8 V following polarization to 5.5V.**

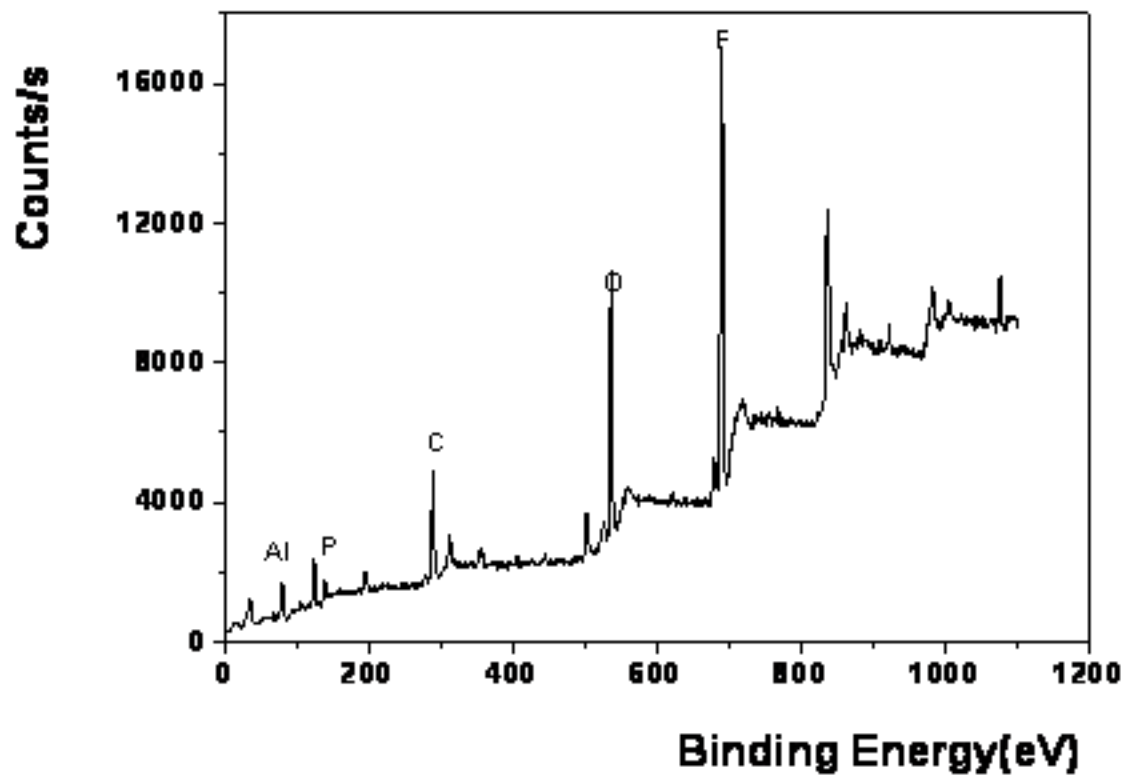


Fig 4a. XPS spectrum of aluminum after anodic polarization in Gen 2 from OCP to 7 V vs Li/Li<sup>+</sup>.

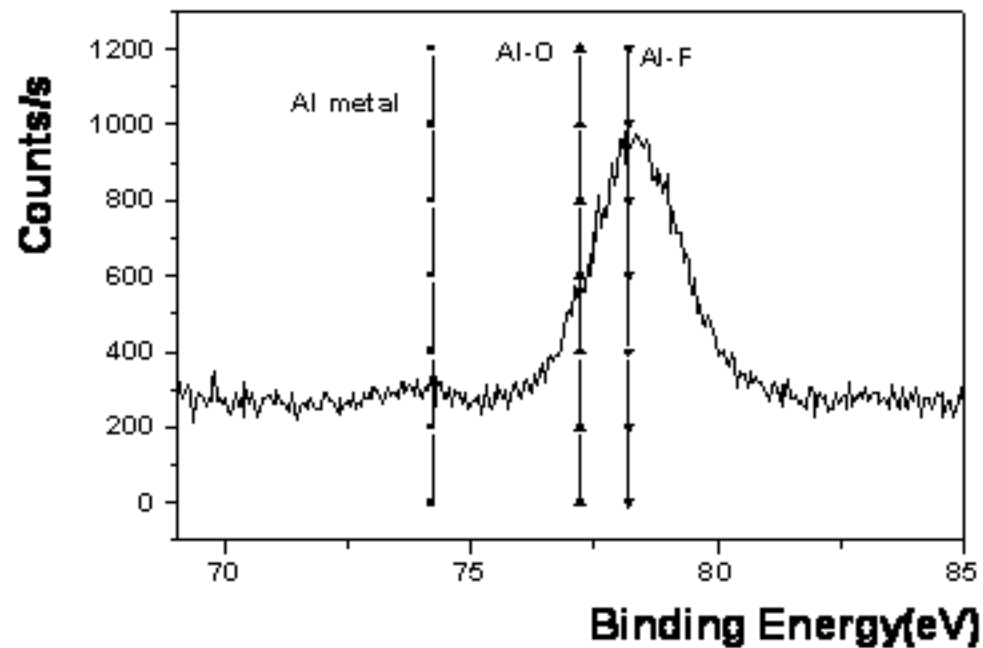


Fig 4b. XPS spectrum of Al 2p for aluminum sample after anodic polarization in Gen 2 from OCP to 7 V vs Li<sup>+</sup>/Li

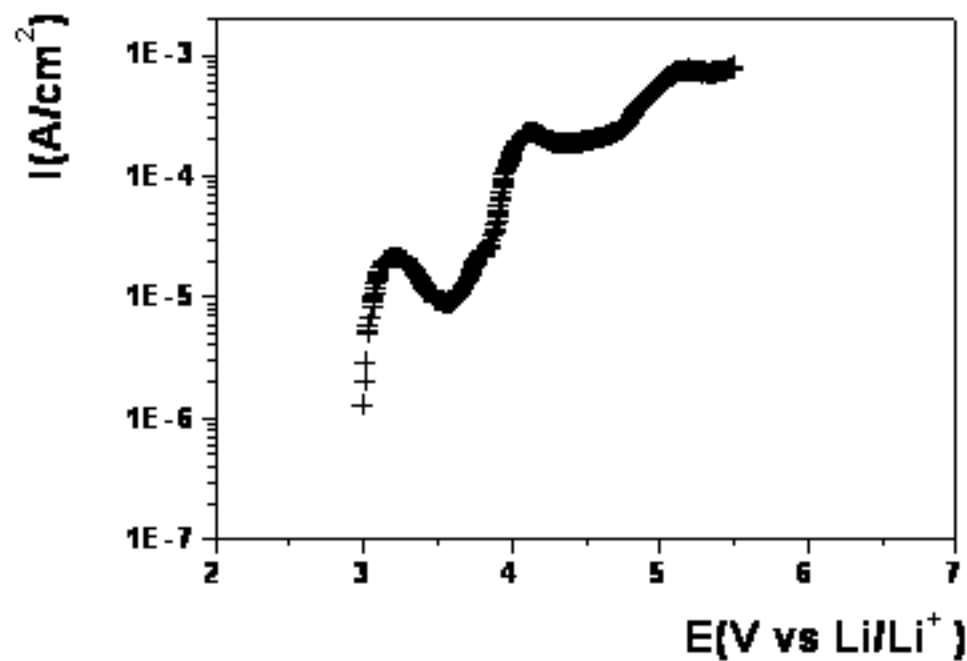


Figure 5. Fourth anodic polarization scan of platinum in 1:1 EC+DMC with 1M  $\text{LiPF}_6$ .